NASA TECHNICAL MEMORANDUM

NASA TM X-62,327

IMPROVEMENTS TO THE KERNEL FUNCTION METHOD OF STEADY, SUBSONIC LIFTING SURFACE THEORY

Richard T. Medan

Ames Research Center
Moffett Field, Calif. 94035

March 1974

TABLE OF CONTENTS

IMPROVEMENTS TO THE KERNEL FUNCTION METHOD OF STEADY, SUBSONIC LIFTING SURFACE THEORY

Richard T. Medan

Ames Research Center

ABSTRACT

This report is concerned with three dimensional, thin wing theory as treated by a kernel function lifting surface method. The method reported herein includes a new technique for the determination of the influence functions. This technique is shown to require fewer quadrature points, while still calculating the influence functions accurately enough to guarantee convergence with an increasing number of spanwise quadrature points. The method also treats control points on the wing's leading and trailing edges. The use of edge control points is compared with usual Multhopp choice of control points and is shown to be advantageous in some respects over the Multhopp choice. The report also deals with wing edge kinks and cranks and methods alternative to the artificial rounding technique for handling them and compares these methods to the artificial rounding technique. Finally, the report introduces and employs an aspect of the kernel function method which apparently has never been used before and which significantly enhances the efficiency of the kernel function approach.

IMPROVEMENTS TO THE KERNEL FUNCTION METHOD OF STEADY, SUBSONIC LIFTING SURFACE THEORY

Richard T. Medan

Ames Research Center

1. INTRODUCTION

This report is concerned with three dimensional, thin wing theory as treated by a kernel function lifting surface method. The method reported herein includes a new technique for the determination of the influence functions. This technique is shown to require fewer quadrature points while still calculating the influence functions accurately enough to guarantee convergence with an increasing number of spanwise quadrature points. The method also treats control points on the wing's leading and trailing edges. The use of edge control points is compared with usual Multhopp choice of control points and is shown to be advantageous in some respects over the Multhopp choice. The report also deals with wing edge kinks and cranks and methods alternative to the artificial rounding technique for handling them and compares these methods to the artificial rounding technique. Finally, the report introduces and employs an aspect of the kernel function method which apparently has never been used before and which significantly enhances the efficiency of the kernel function approach.

2. NOTATION

In this section the principal notation is described. Under certain summation symbols in the text and after certain equations notation such as $J = 1,JJ$ will be found. This notation has been adopted from the FORTRAN computer language and means "for $J = 1$ through JJ."

b	wing span
b_{NK}	coefficient in the expansion for ΔC_p (see eqs. 5.5 – 5.8)
c	local chord length
$\bar{c}$	mean geometric chord, $\int_{-1}^{+1} c^2 d\eta' / \int_{-1}^{+1} c d\eta'$; $\bar{c}$ is used in normalizing the pitching moment and the chordwise center of pressure
ΔC_p	lifting pressure coefficient, $C_{p_l} - C_{p_u}$
$E(m)$	complete elliptic integral of the second kind with parameter m
h_N	chordwise pressure mode (see eq. 5.7)
H_N	influence function (see eq. 5.11)
JJ	number of spanwise integration points (see eq. 7.2.1)
$K(m)$	complete elliptic integral of the first kind with parameter m
K	spanwise pressure mode number
KK	the total number of spanwise pressure modes
M	spanwise control point number
MM	total number of spanwise control points
M_∞	free stream Mach number
N	chordwise pressure mode number
NN	total number of chordwise pressure modes
P	chordwise control point number

PP	total number of chordwise control points
S	the area which is the projection of the wing planform onto the ξ,η plane
W	the wake shed from the trailing edge of S; this wake is assumed to lie in the ξ,η plane and streamlines in the wake are assumed to be parallel to the ξ axis
x	a chordwise variable with origin and scale such that $x = -1$ denotes the leading edge, while $x = +1$ signifies the trailing edge
y	$b\beta(\eta - \eta')/c(\eta')$
α	the slope of the wing surface in the ξ direction
α_{NK}	the downwash created by the Nth chordwise pressure mode and the Kth spanwise pressure mode
β	$\sqrt{1 - M_\infty^2}$
φ	an angular chordwise variable such that $\varphi = 0$ denotes the leading edge, while $\varphi = \pi$ denotes the trailing edge (see eq. 5.8)
ϑ	an angular spanwise variable such that $\vartheta = 0$ denotes the right tip looking upstream, while $\vartheta = \pi$ denotes the left tip (see eq. 5.6)
ϕ	perturbation velocity potential normalized by the free stream speed
ξ,η,ζ	spatial coordinates made nondimensional by the wing semispan (the ξ,ζ plane is chosen parallel to the free stream velocity, while η is the spanwise variable; the wing lies nominally in the ξ,η plane; a prime affixed to any of these variables denotes that it is an integration variable)

Subscripts

le	leading edge
te	trailing edge

3. THE INTEGRAL EQUATION OF LIFTING SURFACE THEORY

The mathematical problem associated with the physical problem being considered is the following:

$$\text{D.E.:} \qquad (1-M_\infty{}^2)\phi_{\xi\xi} + \phi_{\eta\eta} + \phi_{\zeta\zeta} = 0 \tag{3.1a}$$

$$\text{B.C.:} \qquad \phi_\zeta(\xi,\eta,0) = \alpha(\xi,\eta) \quad \text{for } (\xi,\eta) \text{ on } S \tag{3.1b}$$

$$\lim_{\epsilon\to 0}\,[C_p(\xi,\eta+\epsilon) - C_p(\xi,\eta-\epsilon)] = 0 \quad \text{for } (\xi,\eta) \text{ on } W \tag{3.1c}$$

$$\phi \to 0 \quad \text{as the distance from the wing and wake becomes infinite} \tag{3.1d}$$

This boundary value problem can be transformed to an integral equation relating the given downwash to the unknown pressure coefficient difference on the wing (Ashley (1965)). The integral equation for ΔC_p is the following:

$$\alpha(\xi,\eta) = \frac{-1}{8\pi} \lim_{\substack{(\bar\xi,\bar\eta,\bar\zeta)\\ \to(\xi,\eta,0)}} \int_{-1}^{+1} \int_{\xi_{le}}^{\xi_{te}} \frac{\partial}{\partial\bar\zeta} \frac{\bar\zeta \Delta C_p(\xi',\eta')}{(\bar\eta-\eta')^2+\bar\zeta^2} \bar K(\bar\xi-\xi',\beta\sqrt{(\bar\eta-\eta')^2+\zeta^2})\, d\xi'\, d\eta' \tag{3.2}$$

where

$$\bar K(\bar\xi-\xi',\beta\sqrt{(\bar\eta-\eta')^2+\zeta^2}] = 1 + \frac{\bar\xi-\xi'}{\sqrt{(\bar\xi-\xi')^2+\beta^2[(\bar\eta-\eta')^2+\zeta^2]}} \tag{3.3}$$

This equation is the mathematical expression of the fact that ϕ is being represented as a superposition of semi-infinite line doublets. The line doublets have strengths proportional to ΔC_p and have endpoints on the surface S and at downstream infinity.

The meaning of the limit $(\bar\xi,\bar\eta,\bar\zeta)\to(\xi,\eta,0)$ deserves some explanation. If the point $(\xi,\eta,0)$ is in the interior of S or on the trailing edge, then $\bar\xi$ and $\bar\eta$ can simply be set equal to ξ and η, respectively and the limit $\bar\zeta\to 0$ can be performed. If, however, $(\xi,\eta,0)$ is on the leading edge, then $\bar\xi$ cannot be set to ξ_{le} prior to allowing $\bar\zeta$ to approach zero. That this is true can be proven by considering the two dimensional case. In this situation the complex

velocity, $u-iw$, behaves as $1/\sqrt{re^{-i\theta}}$ where r is the distance from the leading edge and $\theta = \tan^{-1}(\zeta/(\xi - \xi_{le}))$. Thus w behaves as $r^{-1/2} \sin\theta/2$ and, therefore, unless $\theta = 2n\pi$, w will approach infinity.

4. FINITE PARTS OF THE DOWNWASH INTEGRAL

The integral in equation 3.2 has to be done numerically, so it is advantageous to be able to interchange the limit processes discussed in the previous section with the integration. It is possible to do this if one takes the so called "finite parts" (Mangler (1951)) of the resultant improper integrals. Integrals which require their finite part to be extracted will be denoted by a cross on the integral sign. The rule to follow for a point not on the leading edge is the following:

$$\oint_{-a}^{+a} \frac{f(\eta)}{\eta^2}\, d\eta = \lim_{\epsilon \to 0} \left[\int_{-a}^{-\epsilon} \frac{f(\eta)}{\eta^2}\, d\eta + \int_{\epsilon}^{a} \frac{f(\eta)}{\eta^2}\, d\eta - \frac{2}{\epsilon} f(0) \right] \tag{4.1}$$

(when $f'(0)$ exists)

That the above rule is equivalent to performing the limit after the integration is easy to show (Mangler (1951)). The rule to use for a point on the leading edge is the following (Mangler (1951)):

$$\oint_{0}^{a} \frac{f(\eta)}{\eta^{3/2}}\, d\eta = \lim_{\epsilon \to 0} \left[\int_{\epsilon}^{a} \frac{f(\eta)}{\eta^{3/2}} - \frac{2}{\epsilon^{1/2}} f(0) \right] \tag{4.2}$$

The equivalence of this rule to performing the limit after the integration has been discussed by Jordan (1967). The proof given by Wagner (1967) is invalid because the wrong sign for an inverse tangent was taken. A simple way to prove the rule would be to simultaneously add the downwash and subtract the downwash integral for an infinite two-dimensional wing swept to the same angle as the leading edge of the given wing. The contribution of both integrands for the interval $\eta - \epsilon$ to $\eta + \epsilon$ can be made to cancel each other, while $\bar{\zeta}$ and $\bar{\xi}$ can be set to 0 and ξ_{le} for the remaining intervals. Furthermore it would be advantageous to use as the two-dimensional wing the one with an infinite chord and with pressure proportional to $1/\sqrt{\xi - \xi_{le}}$ because the downwash on such a wing is zero. The term $-2/\epsilon^{1/2} f(0)$ in equation 4.2 would represent the contribution of one of the outer sections of the two-dimensional wing.

5. THE BASIC METHOD OF SOLUTION

The integral equation can be transformed to a more convenient form by the following transformations of the chordwise variables:

$$x' = \frac{b}{c(\eta')}\left[\xi' - \frac{\xi_{le}(\eta') + \xi_{te}(\eta')}{2}\right] \tag{5.1}$$

$$x = \frac{b}{c(\eta')}\left[\xi - \frac{\xi_{le}(\eta') + \xi_{te}(\eta')}{2}\right] \tag{5.2}$$

Then, with the finite part notation of the previous section, equation 3.2 becomes:

$$\alpha(\xi,\eta) = -\frac{1}{8\pi} \int\!\!\!\!\!\!\diagup_{-1}^{+1} \frac{c(\eta')}{b} \int_{-1}^{+1} \Delta C_p(\xi',\eta')\bar{K}(x-x',y)\,dx'\,d\eta' \tag{5.3}$$

where

$$y = \frac{b\beta}{c(\eta')}(\eta - \eta') \tag{5.4}$$

The technique used to obtain a solution to equation 5.3 is the collocation method. In this method the unknown pressure distribution is expressed as the sum of a finite number of assumed functions with unknown, constant coefficients. The coefficients are determined by enforcing equation 5.3 at a finite set of (ξ,η) points and solving a set of linear, algebraic equations obtained thereby.

The expansion for the pressure is as follows:

$$\Delta C_p = \frac{2b}{c(\eta')} \sum_{K=1}^{KK} \sum_{N=1}^{NN} \sin K\vartheta' h_N(x') b_{NK} \tag{5.5}$$

where

$$\vartheta' = \cos^{-1}\eta' \tag{5.6}$$

$$h_N(x') = \begin{cases} \dfrac{2}{\pi}\sqrt{\dfrac{1-x'}{1+x'}} = \dfrac{2}{\pi}\cot\dfrac{\varphi}{2} & \text{for } N=1 \quad (5.7a) \\ \dfrac{2}{\pi}\sin[(N-1)\varphi] & \text{for } N>1 \quad (5.7b) \end{cases}$$

and where

$$\varphi = \cos^{-1}(-x') \tag{5.8}$$

Substituting the pressure expansion into the integral equation (eq. 5.3) gives:

$$\alpha(\xi,\eta) = \sum_{K=1}^{KK}\sum_{N=1}^{NN} \alpha_{NK}(\xi,\eta)\, b_{NK} \tag{5.9}$$

where

$$\alpha_{NK}(\xi,\eta) = \frac{-1}{2\pi}\oint_{-1}^{+1} \frac{\sin K\vartheta'}{(\eta-\eta')^2}\, H_N(x,y)\, d\eta \tag{5.10}$$

and where

$$H_N(x,y) = \frac{1}{2}\int_{-1}^{+1} h_N(x')\,\bar{K}(x-x',y)\, dx' \tag{5.11}$$

The function H_N in the above equation is called the influence function. The behavior of this function for small y deserves careful consideration, but the discussion of its behavior is deferred to section 7.4. If equation 5.10 is enforced at a set of collocation or control points denoted by (ξ_P,η_M), then the following set of simultaneous equations for the unknown coefficients, b_{NK}, is obtained:

$$\alpha_{PM} = \alpha_{PMNK}\, b_{NK} \tag{5.12}$$

where

$$\alpha_{PM} = \alpha(\xi_P,\eta_M)$$

and

$$\alpha_{PMNK} = \alpha_{NK}(\xi_P, \eta_M)$$

In the above equation, the index P ranges from 1 to PP while M ranges from 1 to MM. Generally PP is made equal to NN and MM is equated to KK. In this paper the set of numbers α_{PMNK} is called the influence matrix or the set of downwash modes.

6. WING EDGE KINKS AND CRANKS

The pressure coefficient expansion in eq. 5.5 behaves near the leading edge as the reciprocal of the square root of the distance from the leading edge; near the trailing edge as the square root of the distance to the trailing edge; and near the side edges as the square root of the distance to the side edge. This behavior is correct at the leading and trailing edges if there is no kink or crank in the edge as shown by Landahl (1968). If there is a kink or crank, then the character of the pressure distribution changes considerably (Rossiter (1969)). The pressure behaves as the distance to the kink or crank raised to some power which is a function of the sweep angles to either side of the kink or crank and is not known in closed form. Furthermore, even if the exponent could be determined easily, it would be very difficult to correct the pressure expansion. This is because the pressure modes in eq. 5.5 produce downwash modes which are logarithmically singular at the spanwise location of the kink or crank, except when $\xi = \xi_{le}(\eta)$ or $\xi = \xi_{te}(\eta)$. Thus each and every pressure mode must be modified near the spanwise location of a kink or crank. This situation is to be contrasted with the case where one is trying to correct the pressure expansion for the effects of a slightly deflected control surface. In the latter instance the pressure modes in eq. 5.5 do not produce singular downwash modes and, consequently, one can correct the pressure expansion merely by adding a control surface pressure mode to the expansion (Medan (1973)). Such a procedure is not valid for correcting the pressure expansion for kink effects. In view of the difficulties of determining pressure modes appropriate for kinked and cranked wings, the usual procedure taken is to introduce artificial rounding of the kinks (Garner (1968)). An alternate approach is to avoid putting interior control points at or very near kink stations. This can be done either by deleting the interior points which are at or near kink stations or by avoiding the kink stations altogether. When the approach of deleting the interior points is adopted, then at least the same number of pressure modes must be deleted. The procedure used herein is to decrease KK (eq. 5.9). When this is done there are sometimes more equations left than unknowns and this requires that the solution be obtained in the sense of least squares. Both methods of avoiding the kink locations have been used and are compared with the artificial rounding technique in section 9.3.

7. CALCULATION OF THE DOWNWASH MODES

In order to effectively calculate the downwash modes of eq. 5.10 efficient numerical methods must be developed to calculate the chordwise integral (influence function) of eq. 5.11 and the spanwise integral of eq. 5.10.

7.1 Method of Chordwise Integration

The first step in the calculation of the downwash modes is to calculate the influence functions of eq. 5.11. When $y = 0$, the integrations are easily done analytically, but when $y \neq 0$, the integrations are done numerically. In the latter case the influence functions could be expressed in terms of elliptic integrals of the first, second, and third kinds, but since the elliptic integrals themselves must be calculated numerically and since the elliptic integral formulation involves numerical problems, a numerical calculation method specifically tailored to the influence functions is preferred. In the subject method the following transformation of variable is used:

$$x' = -\cos\varphi' \tag{7.1.1}$$

Equation 5.11 then becomes

$$H_N(x,y) = \frac{1}{2}\int_o^\pi h_N(x')\bar{K}(x-x',y)\sin\varphi'\,d\varphi' \tag{7.1.2}$$

Because of the appearance of $\sin\varphi'$, the leading edge singularity of $h_1(x')$ is cancelled, leaving a finite integrand at $\varphi' = 0$. This in turn allows the trapezoidal rule to be used to evaluate eq. 7.1.2. The simplicity of this rule is deceptive since it is actually extremely accurate if the integrand is a polynomial in x'. It can be shown (Hildebrand (1956)) that if L integration points are used, then exact results will be obtained if the integrand is a polynomial with degree as large as $2L - 1$. The product of $h_N(x')$ with $\sin\varphi'$ is a polynomial in x' of degree N, so the degree of representation remaining for $\bar{K}$ is $2L - N - 1$.

The degree of accuracy needed in the chordwise integration is determined by the weight given to the influence function in the spanwise integration, as will be shown in section 7.3. However, the question of how large L should be in order to give the specified degree of accuracy

without being unnecessarily large cannot be answered by simple formulas. Instead the answer is self-generated by the computer subroutine which performs the chordwise integration. This is accomplished by computing the integrals with increasingly larger values of L, comparing the changes in the computed integrals, and stopping when the increments become smaller than a δ computed by the calling program. This algorithm assumes the increment to be a reliable measure of the accuracy. This is not always true when y and L are both small, so it was found necessary to prescribe a minimum value of L based on y. At first glance it may seem that this process of integrating over and over would be very inefficient in terms of computer time, but the simplicity of the chordwise quadrature formula offers a saving grace. The redeeming quality is that the integration points for $L = 2J$ contain as a subset the integration points for $L = J$ and the weights for the two different values of L are in constant proportion. This means that the result for $L = 2J$ can be obtained by computing the integrand at only J points and by using the previously computed integral (the one computed with J points total). This involves only slightly more computing than if the result were obtained only for $L = 2J$ and it gives the needed information on the convergence. Thus this reintegrating procedure is not inefficient.

7.2 Method of Spanwise Integration

The integral in eq. 5.10 is computed by Multhopp's famous integration formula (Multhopp (1950)), which is as follows:

$$-\frac{1}{2\pi}\int_{-1}^{1}\frac{f(\eta')}{(\eta-\eta')^2}\,d\eta' \cong \sum_{J=1,JJ} B_J(\eta) f(\eta_J') \tag{7.2.1}$$

where

$$\eta'_J = \cos\vartheta_J = \cos\frac{J\pi}{JJ+1} \tag{7.2.2}$$

If η is chosen to be one of the integration stations (the M-th station, for example), then the formula for the Multhopp quadrature weights is

$$B_J(\eta) \equiv B_{MJ} = \begin{cases} \dfrac{JJ+1}{4\sin\vartheta_M} & M = J \qquad (7.2.3a) \\ \dfrac{-\sin\vartheta_J}{(JJ+1)(\eta_M-\eta_J)^2} & |M-J| \text{ odd} \qquad (7.2.3b) \\ 0 & |M-J| \text{ even} \qquad (7.2.3c) \end{cases}$$

When $|M-J|$ is small and JJ is large, the following approximation holds:

$$B_{MJ} \cong \frac{-(JJ+1)}{(M-J)^2\pi^2 \sin\vartheta_M} \qquad |M-J| \text{ odd} \tag{7.2.4}$$

7.3 Choosing δ for Chordwise Integrator

One can observe from equation 7.2.3 that the quadrature weights vary considerably in going from the integration stations farthest from the control station to those nearest. The significance of this fact as it pertains to the δ given to the chordwise integrator (sec. 7.1) is that δ should vary with the spanwise integration station. One can also observe from equation 7.2.4 that the quadrature weights nearest the control station increase in proportion to $JJ+1$. The importance of this behavior is (1) if the chordwise integration were done with a fixed accuracy, the computed answer would ultimately diverge and (2) δ should be decreased as JJ is increased. A final fact needs to be introduced before the rule for selecting δ is given. This is that the number of points, L, required to obtain a given accuracy increases significantly as y becomes small (i.e., as B_{MJ} becomes large with JJ fixed). This last observation is the reason for the appearance of ϵ in the following formula for δ (if the accuracy did not vary with y, hence with B_{MJ}, ϵ would be replaced with 1):

$$\delta = \frac{\delta_0}{(JJ+1)^2(-B_{MJ})^{\epsilon}} \tag{7.3.1}$$

In the above, δ_0 is constant for a given planform, but should vary with the aspect ratio since the value of JJ required to yield a given accuracy increases with the aspect ratio. For all results reported herein $\delta_0 = AR^2$ and $\epsilon = .5$ unless otherwise stated. These choices for δ_0 and ϵ are the results of a modest attempt to minimize the total number of integration points and a better choice might still be determined.

Some results have been obtained for the downwash created by two of the pressure modes on two different wings. These results are shown in Table 7.3.1 which compares the total number of integration points used by the current method with the number which would be used by two other methods (Wagner (1967) and Zandbergen (1967)) provided that they use the Multhopp spanwise integration method. It can be seen that the current method uses substantially fewer points than the others while still converging to the correct answers.

Another set of results is given in Table 7.3.2 as an illustration of the instability which will occur if the chordwise integration is not coupled to the spanwise integration in the manner of equation 7.3.1. The results for this table were obtained by not allowing more than 24 chordwise integration points to be used.

7.4 Corrections for Spanwise Singularities

Although Multhopp's integration formula handles the 2nd order pole singularity, the influence function contains singularities which Multhopp's formula either cannot handle or else cannot handle effectively. For control points not on the wing edges the influence functions contain terms behaving as $(\eta - \eta')^2 \ln|\eta - \eta'|$. The factor $(\eta - \eta')^2$ is cancelled by its reciprocal in equation 5.10 leaving a logarithm, which is not handled efficiently by Multhopp's formula. The technique used to alleviate this deficiency is that used by Mangler (1952) in which terms which will cancel the logarithm (leaving only $(\eta - \eta')^3 \ln|\eta - \eta'|$ terms) are simultaneously added and subtracted from the integrand. The added part is integrated analytically while the remainder is treated by Multhopp's formula. The explicit formula thus obtained for the downwash is:

$$\alpha_{KN}(\xi,\eta) = \frac{1}{2}\left(\frac{b\beta}{c(\eta)}\right)^2 \frac{dh_N}{dx'}\bigg|_{x'=x} I_K(\eta) - \frac{1}{2\pi}\int_{-1}^{+1} \frac{\sin K\vartheta'}{(\eta-\eta')^2}\left\{H_N(\xi,\eta,\eta')\right.$$

$$\left. + \frac{1}{2}\left(\frac{b\beta}{c(\eta)}\right)^2 \frac{dh_N}{dx'}\bigg|_{x'=x} (\eta-\eta')^2 \ln|\eta-\eta'|\right\} d\eta' \qquad (7.4.1)$$

where

$$I_K(\eta) = \frac{1}{2\pi}\int_{-1}^{+1} \sin K\vartheta' \ln|\eta-\eta'|\, d\eta'$$

$$= \begin{cases} \frac{1}{8}\left[2\eta^2 - 1 - \ln 4\right] & K = 1 \quad \text{(Mangler (1952))} \qquad (7.4.2a) \\ -\frac{1}{16}\frac{1}{K^2-1}\left[K \sin K\vartheta \sin\vartheta + \cos K\vartheta \cos\vartheta\right] & K > 1 \qquad (7.4.2b) \end{cases}$$

(Zandbergen (1967))

and where

$$\vartheta = \cos^{-1} \eta \tag{7.4.2c}$$

The integral appearing in equation 7.4.1 is determined by Multhopp's formula. The importance of this correction has been shown by Garner (1966).

For control points on the leading and trailing edges the behavior of the influence functions changes considerably. This behavior has been discussed by Jordan (1967), who also has given a method to derive the appropriate formulas (1969). For a control point on the leading edge the leading terms in the expansions for the influence functions are proportional to $|\eta - \eta'|^{1/2}$ and these are followed by ones proportional to $|\eta - \eta'|^{3/2}$. At the trailing edge the leading terms are constants, which can be disregarded, followed by terms proportional to $|\eta - \eta'|^{3/2}$. By expanding the influence functions in the manner of Jordan and by adding and subtracting the 1/2 and 3/2 order terms and by using equation 4.2 the following formula for the downwash for points on the leading edge has been derived:

$$\begin{aligned}
\alpha_{NK}(\xi,\eta) = {} & g_N^{\,l} \cos[(K-1)\vartheta]\,[J_0^{\,l-}(\eta)\Gamma_3^{-}(\eta) + J_0^{\,l+}(\eta)\Gamma_3^{+}(\eta)] \\
& + g_N^{\,l}\,\frac{(K-1)\sin[(K-1)\vartheta]}{\sin\vartheta}\,[-J_0^{\,l-}(\eta)\Gamma_1^{-}(\eta) + J_0^{\,l+}(\eta)\Gamma_1^{+}(\eta)] \\
& - \frac{1}{2}\,g_N^{\,l}\cos[(K-1)\vartheta]\,\frac{b}{2c(\eta)}\,[(\tan\lambda_{le}^{-} - \tan\lambda_{te}^{-})J_0^{\,l-}(\eta)\Gamma_1^{-}(\eta) \\
& + (\tan\lambda_{le}^{+} - \tan\lambda_{te}^{+})J_0^{\,l+}(\eta)\,\Gamma_1^{+}(\eta)] \\
& + g_N^{\prime\,l}\cos[(K-1)\vartheta]\,[J_1^{\,l-}(\eta)\,\Gamma_1^{-}(\eta) + J_1^{\,l+}(\eta)\,\Gamma_1^{+}(\eta)] \\
& - \frac{1}{2\pi}\int_{-1}^{+1}\frac{1}{(\eta-\eta')^2}\Big\{\sin\vartheta'\cos[(K-1)\vartheta']H_N(\xi,\eta,\eta') \\
& - \Delta\Big(\sin\vartheta'\cos[(K-1)\vartheta']H_N(\xi,\eta,\eta')\Big)\Big\}d\eta'
\end{aligned} \tag{7.4.3}$$

where

$$g_N{}^l = \begin{cases} \frac{2}{\pi} & N = 1 \quad (7.4.4a) \\ 0 & N > 1 \quad (7.4.4b) \end{cases}$$

$$g'_N{}^l = \begin{cases} -\frac{1}{\pi} & N = 1 \quad (7.4.5a) \\ \frac{4}{\pi}(N-1) & N > 1 \quad (7.4.5b) \end{cases}$$

$$J_0{}^{l\pm}(\eta) = 4\left[\frac{b\beta}{2c(\eta)\cos\phi_{le}^{\pm}}\right]^{1/2}[E(m_l^{\pm}) + (m_l^{\pm} - 1)K(m_l^{\pm})] \quad (7.4.6a,b)$$

$$J_1{}^{l\pm}(\eta) = \frac{4}{3}\left[\frac{b\beta}{2c(\eta)\cos\phi_{le}^{\pm}}\right]^{3/2}[(2m_l^{\pm} - 1)E(m_l^{\pm}) + (1 - m_l^{\pm})K(m_l^{\pm})] \quad (7.4.7a,b)$$

$$m_l^{\pm} = \frac{1}{2}(1 + \sin\phi_{le}{}^{\pm}) \quad (7.4.8a,b)$$

$$\phi_{le}{}^{\pm} = \tan^{-1}\left[\frac{1}{\beta}\tan\lambda_{le}{}^{\pm}\right] \quad (7.4.9a,b)$$

$$\Gamma_3{}^{\pm}(\eta) = \frac{\sqrt{2}}{\pi}[2E(\bar{m}^{\pm}) - K(\bar{m}^{\pm})] \quad (7.4.10a,b)$$

$$\Gamma_1{}^{\pm}(\eta) = \frac{-2\sqrt{2}}{3\pi}[(2\bar{m}^{\pm} - 1)E(\bar{m}^{\pm}) + (1 - \bar{m}^{\pm})K(\bar{m}^{\pm})] \quad (7.4.11a,b)$$

$$\bar{m}^{\pm} = \frac{1 \mp \eta}{2} \quad (7.4.12a,b)$$

$$\Delta\left(\sin\vartheta'\cos[(K-1)\vartheta']\,H_N(\xi,\eta,\eta')\right) = \begin{cases} \Delta^-\left(\sin\vartheta'\cos[(K-1)\vartheta']\,H_N(\xi,\eta,\eta')\right) & \eta' < \eta \quad (7.4.13a) \\ \Delta^+\left(\sin\vartheta'\cos[(K-1)\vartheta']\,H_N(\xi,\eta,\eta')\right) & \eta' > \eta \quad (7.4.13b) \end{cases}$$

$$\Delta^{\pm}\left(\sin\vartheta' \cos\left[(K-1)\vartheta'\right] H_N(\xi,\eta,\eta')\right) = g_N{}^{l} J_0{}^{l\pm}(\eta) \cos\left[(K-1)\vartheta\right] \sin\vartheta' \left|\eta-\eta'\right|^{1/2}$$

$$+ \left\{ \pm g_N{}^{l} J_0{}^{l\pm}(\eta) \frac{(K-1)\sin\left[(K-1)\vartheta\right]}{\sin\vartheta} - \frac{1}{2} g_N{}^{l} J_0{}^{l\pm} \cos\left[(K-1)\vartheta\right] \frac{b}{2c(\eta)} \right.$$

$$\left. \times \left(\tan\lambda_{le}{}^{\pm} - \tan\lambda_{te}{}^{\pm}\right) + g_N'{}^{l} J_1{}^{l\pm}(\eta) \cos\left[(K-1)\vartheta\right] \right\} \sin\vartheta' \left|\eta-\eta'\right|^{3/2} \qquad (7.4.14a,b)$$

In the above formulas $\lambda_{le}{}^{\pm}$ and $\lambda_{te}{}^{\pm}$ are the leading and trailing edge sweep angles. The angles are defined such that they are positive on the side of the control point which is swept forward and such that $\lambda_{le}{}^{+} = -\lambda_{le}{}^{-}$ and $\lambda_{te}{}^{+} = -\lambda_{te}{}^{-}$ for an unkinked wing. Also it should be noted that in the above equations the spanwise pressure modes have been changed from $\sin K\vartheta'$ to $\sin\vartheta' \cos\left[(K-1)\vartheta'\right]$. The reason is that the latter modes are better conditioned numerically. After the downwash modes are calculated they are linearly transformed to make them correspond to the pressure modes of equation 5.5. The functions $J_0{}^{l\pm}(\eta)$ and $J_1{}^{l\pm}(\eta)$ are spanwise integrals, which may be determined by equations 7.4.3 and 7.4.13. $J_0{}^{l\pm}(\eta)$ was determined by use of equation 4.2 (S. W. Wagner, unpublished notes). The above formulas account for the spanwise variation of the spanwise pressure modes (2nd term of eq. 7.4.3) and wing chord (3rd term of eq. 7.4.3) but not for curvature of the wing leading edge.

The formulas for points on the trailing edge are as follows:

$$\alpha_{NK}(\xi,\eta) = -g_N{}^{t} \cos\left[(K-1)\vartheta\right] \left[J_1{}^{t-}(\eta)\,\Gamma_1{}^{-}(\eta) + J_1{}^{t+}(\eta)\,\Gamma_1{}^{+}(\eta)\right]$$

$$- \frac{1}{2\pi} \int_{-1}^{+1} \frac{1}{(\eta-\eta')^2} \left\{ \sin\vartheta' \cos\left[(K-1)\vartheta'\right] H_N(\xi,\eta,\eta') \right.$$

$$\left. - \Delta\left(\sin\vartheta' \cos\left[(K-1)\vartheta'\right] H_N(\xi,\eta,\eta')\right) \right\} d\eta' \qquad (7.4.15)$$

$$g_N{}^{t} = \begin{cases} \dfrac{2}{\pi} & N = 1 \qquad (7.4.16a) \\ \dfrac{4}{\pi}(-1)^N (N-1) & N > 1 \qquad (7.4.16b) \end{cases}$$

$$J_1^{t\pm}(\eta) = \frac{4}{3}\left[\frac{b\beta}{2c(\eta)\cos\phi_{te}^{\pm}}\right]^{3/2}\left[(2m_t^{\pm}-1)E(m_t^{\pm})+(1-m_t^{\pm})K(m_t^{\pm})\right] \tag{7.4.17a,b}$$

$$m_t^{\pm} = \frac{1}{2}\left[1-\sin\phi_{te}^{\pm}\right] \tag{7.4.18a,b}$$

$$\phi_{te}^{\pm} = \tan^{-1}\left[\frac{1}{\beta}\tan\lambda_{te}^{\pm}\right] \tag{7.4.19a,b}$$

$$\Delta\left(\sin\vartheta'\cos\left[(K-1)\vartheta'\right]H_\eta(\xi,\eta,\eta')\right) = \begin{cases} \Delta^-\left(\sin\vartheta'\cos\left[(K-1)\vartheta'\right]H_\eta(\xi,\eta,\eta')\right) & \eta'<\eta \quad (7.4.20a) \\ \Delta^+\left(\sin\vartheta'\cos\left[(K-1)\vartheta'\right]H_\eta(\xi,\eta,\eta')\right) & \eta'>\eta \quad (7.4.20b) \end{cases}$$

$$\Delta^{\pm}\left(\sin\vartheta'\cos\left[(K-1)\vartheta'\right]H_N(\xi,\eta,\eta')\right) = -g_N^t J_1^{t\pm}\cos\left[(K-1)\vartheta'\sin\vartheta'\right]\left|\eta-\eta'\right|^{3/2} \tag{7.4.21a,b}$$

The importance of these corrections for a control surface pressure mode which is similar near the wing edges to the pressure modes discussed herein for $N>1$ was established by Medan (1973). When $N=1$, the numerical integration would not even converge without these corrections because of the $-3/2$ order singularity, which cannot be handled with Multhopp's integration formula.

K	AR	N	JJ	α_{NK}	ERROR IN CHORDWISE INTEGRATION	ERROR IN SPANWISE INTEGRATION	NUMBER OF POINTS USED OR WHICH WOULD BE USED		
							CURRENT METHOD	NLR (ref.11)	WAGNER (ref.4)
1	2	1	15	1.33572	$<5X10^{-6}$	-0.00101	84	252	232
			31	1.33661	$<5X10^{-6}$	-0.00012	192	868	536
			63	1.33672	$<5X10^{-6}$	-0.00001	480	1888	1336
			127	1.33673	$<5X10^{-6}$	$<5X10^{-6}$	1368	3312	2336
			255	1.33673	$<5X10^{-6}$	$<5X10^{-6}$	3264	>5746	4206
			∞[1]	1.33673	--	--	--	--	--
		7	15	-0.55496	-0.00017	-0.07454	same as for N=1		
			31	-0.49314	0.00001	-0.01272			
			63	-0.48212	$<5X10^{-6}$	-0.00170			
			127	-0.48063	$<5X10^{-6}$	-0.00021			
			255	-0.48044	$<5X10^{-6}$	-0.00002			
			∞[2]	-0.48042	--				
	6	1	15	2.48865	$<5X10^{-6}$	-0.02105	42	148	232
			31	2.50220	$<5X10^{-6}$	-0.00750	108	348	464
			63	2.50841	$<5X10^{-6}$	-0.00129	252	774	928
			127	2.50956	$<5X10^{-6}$	-0.00014	588	1626	1928
			255	2.50968	$<5X10^{-6}$	-0.00002	1332	3508	3784
			∞[1]	2.50970	$<5X10^{-6}$	--	--	--	--
		7	15	-3.12098	-0.00146	-1.684	same as for N=1		
			31	-1.94368	-0.00001	-0.507			
			63	-1.54671	$<5X10^{-6}$	-0.110			
			127	-1.45384	$<5X10^{-6}$	-0.017			
			255	-1.43927	$<5X10^{-6}$	-0.002			
			∞[2]	-1.437	--	--			

1. Kellaway, W.: Evaluation of the Downwash Integral for Rectangular Planforms by the BAC Subsonic Lifting Surface Method. Aeronautical Quarterly, vol. 23, pp. 181-187, August 1972.
2. extrapolated

TABLE 7.3.1. – DOWNWASH ON RECTANGULAR WINGS AT $\xi = 0.8c/(b/2)$ AND $\eta = 0.0$ DUE TO PRESSURE MODES OF EQ. 5.5. The starting number of chordwise integration points was 2.

JJ	α_{11}	ERROR
15	1.33572	-0.00101
31	1.33662	-0.00011
63	1.33784	0.00110
127	1.36127	0.02454
255	1.51481	0.17808

TABLE 7.3.2. DOWNWASH ON AN ASPECT RATIO 2 RECTANGULAR WING AT $\xi = 0.8c/(b/2)$ AND $\eta = 0$ DUE TO THE $N = K = 1$ PRESSURE MODE AND WITH NUMBER OF CHORDWISE INTEGRATION POINTS LIMITED TO 24.

8. CHOICE OF CONTROL POINTS

The set of control points (also called collocation points) is discussed in this section.

8.1 Selection of Chordwise Control Points

Multhopp (1950) gave a general rule for determining where the chordwise control points should be placed. Hsu (1959) has shown that this choice is optimal in the sense that the choice will lead to the exact answer for the i-th moment of the pressure in the two-dimensional airfoil case when the camber line is a polynomial of degree $2PP - 1 - i$ or less. PP is the number of chordwise control points and the number of pressure modes. This rule is the following:

$$x_P = -\cos\frac{2\pi P}{2PP+1} \qquad P = 1, PP \tag{8.1.1}$$

Thus, for example, the exact lift ($i = 0$) and pitching moment ($i = 1$) would be obtained in the two dimensional case if 5 points were placed according to the above rule and the camberline were a polynomial of degree 8 or less. Jordan (1969), however, has pointed out that a rule such as the above is not necessarily the best in the three dimensional case and that advantage can be realized by using control points on the wing edges. One reason given by Jordan is that the edge control points become ideal as the aspect ratio approaches zero. Another reason is that with edge control points the remaining logarithmic term (the $(\eta - \eta')^3 \ln|\eta - \eta'|$ of section 7.4), which is a major source of error, can be eliminated in favor of a less troublesome one (proportional to $|\eta - \eta'|^{5/2}$). Wagner has shown (unpublished work) that the following choice, which includes control points on the leading and trailing edges, is optimal in the previously discussed sense:

$$x_P = -\cos\frac{(P-1)\pi}{PP-1} \qquad P = 1, PP \tag{8.1.2}$$

The degree of precision for Wagner's rule is 2 less than for Multhopp's rule because 2 control point locations are preassigned.

These two choices for the chordwise control points are compared in section 9.

8.2 Spanwise Control Points

Although Multhopp's integration formula (eq. 7.2.1) does not impose any conditions on the spanwise control point locations, it is advantageous to choose the spanwise control point locations to be a subset of the integration points. The reason is that with this restriction almost half of the quadrature coefficients are zero (see eq. 7.2.3c). Thus the influence functions need to be determined for fewer times. The following rule will insure that the spanwise control points are a subset of the spanwise integration points provided that $(JJ + 1) = q(MM + 1)$ where q is an integer:

$$\eta_M = \cos \frac{M\pi}{MM + 1} \qquad M = 1, MM \tag{8.2.1}$$

This choice of control points has been used for most kernel function methods and is employed in the current method with only minor variations although the computer programs associated with the method allow any of the spanwise integration points to be used as spanwise control points.

9. RESULTS

In this section results for several wing planforms are presented and discussed and compared with other theoretical results. These results were calculated using the computer programs documented in Medan (1973*b-e*, 1974, 1974*b*).

9.1 The Aspect Ratio 2 Rectangular Wing

The influences of the number of spanwise integration points, JJ, the number of chordwise control points, NN, and the type of control point distribution on the predicted lift curve slope are shown in figures 9.1.1 and 9.1.2. For these results $MM = KK = 7$ and $PP = NN$. Figure 9.1.1(a) shows the results for the Wagner control point distribution (eq. 8.1.2) for various values of PP from 3 to 7. Figure 9.1.1(b) shows similar results for the Multhopp control point distribution (eq. 8.1.1). A comparison of these figures reveals that as JJ approaches infinity, the Multhopp distribution gives more accurate answers for a given value of PP. However, the Wagner distribution results converge much faster with respect to JJ so that for finite values of JJ, the Wagner distribution generally gives better results. The reason for this is that, aside from control points exactly on the wing edges, the Wagner points are a much greater distance from the edges than the Multhopp points and the remaining irregularities not removed from the spanwise integrals (section 7.4) become large as the edges are approached. Thus the Wagner distribution is sometimes superior to the Multhopp distribution in terms of accuracy. It will be shown the next section that it is also superior in terms of efficiency.

Some of the points in figure 9.1.1 have been replotted in figure 9.1.2 to show more clearly the differences between results obtained with the Wagner distribution and results obtained using the Multhopp distribution. This plot also shows the high degree of accuracy that can be obtained with the kernel function method. All of the points on this graph fall within .062% of the exact answer, which is estimated to be $2.47440 \pm .00002$. Furthermore all of the points for $JJ \geq 127$ fall within .015% of the exact answer and the points for $N = 5$ and $JJ = 255$ are within .004% of the exact answer. Note that these results were obtained with only 16 to 20 unknowns.

Figure 9.1.3 compares the present kernel function method to the Multhopp method reported by Lamar (1968). The present method employed the Multhopp points for a meaningful comparison. This graph shows that 4 chordwise modes and 2 symmetric spanwise modes are

sufficient to give a very accurate answer. The results of Lamar (1968) were obtained by using the same set of control points and pressure modes mutually dependent with the ones used herein. Therefore the large discrepancy between the two sets of results is due to the integration procedures employed to determine the elementary downwash modes (influence coefficient matrix). In particular the divergence of the Multhopp method as MM goes to infinity is due to the fact that a fixed number of chordwise integration points is employed by Lamar, i.e., the chordwise integration is not coupled to the spanwise integration as discussed in section 7. The poorness of the results obtained for $MM = 3$ and $MM = 7$ is probably due mainly to the fact that not enough spanwise integration points were employed. In the Multhopp method the spanwise integration points are identical with the spanwise control points, i.e., $JJ = MM$, so only 3 or 7 spanwise integration points were employed. In the precomputer era in which Multhopp formulated his method such a limitation was very advantageous and very nearly essential, but with the current high speed computers and the attendant quest for increased accuracy such a limitation is a distinct disadvantage, as figure 9.1.3 shows.

9.2 The Circular Wing

The circular wing has been treated at length by Jordan (1971), who has given sufficiently accurate numerical values to compare against. Results using the current method with 36 different combinations of PP, MM, and JJ and using the Wagner chordwise control point distribution have been calculated and are tabulated in tables 9.2.1 - 9.2.5. The lift curve slope is given in table 9.2.1 from which it can be seen that C_{L_α} is predicted with an error of less than .001% for $PP = 7$, $MM = 15$, and $JJ = 255$. Furthermore the largest error for any of the cases is only .72%. One can also see from this table and also following tables that PP and MM need not be related to one another as is suggested by Lamar (1968). The reason that these quantities (N and M in Lamar (1968)) need to be related for Lamar's method is partly due to the fact that the spanwise integration stations and spanwise control points are identical. This requires MM (M) to be increased as PP (N) is increased because more integration points are needed as PP increases. Thus the point is reached where either an unacceptably large number of unknowns is involved or else the computer storage capacity is exceeded. The current method is not hampered by this problem as the tables show.

The vortex drag factor is presented in table 9.2.2. The exact result for this quantity was not given by Jordan.

Table 9.2.3 gives the results for the pitching moment. Again the result for the case $PP = 7$, $MM = 15$, and $JJ = 255$ is extremely accurate being in error by only $-.0030\%$. In the worst case the error is only .77%.

The calculated chordwise center of pressure is shown in table 9.2.4. As for the previous results the error for the case $PP = 7$, $MM = 15$, and $JJ = 255$ is very small ($-.0040\%$) while in the worst case the error is still only 0.67%.

The sectional lift coefficient at the wing tip is shown in table 9.2.5. The calculated results in this instance are not nearly as good as the results obtained for the overall parameters. An examination of the table shows that more spanwise control points should have been used. The fundamental problem, however, consists in the fact that there are singularities in the pressure distribution which are not present in the pressure modes of eqs. 5.5 - 5.7. In particular Jordan (1971) has shown that the sectional lift is given by

$$c_l(\eta) = \left[1 + \frac{1}{16}\sqrt{1-\eta^2}\ \ln\frac{4}{1-\eta^2}\right] c_l(1) + O(\sqrt{1-\eta^2})$$

while the pressure modes of eqs. 5.5 - 5.7 admit only a representation of the form

$$c_l(\eta) = A_0 + A_1\,\eta + \cdots + A_{KK-1}\,\eta^{KK-1}$$

This inadequacy in the present theory, however, is not very significant because the sectional loading itself, which is proportional to the product of the section lift coefficient with the chord, goes to zero at the tip.

Table 9.2.6 compares the present method with other methods (Labrujere (1968), Giesing (1968), and Mercer (1973)). The method of Garner is quite similar to the current method and, for the same parameters, yields essentially the same results. The present method differs from Garner's principally in the manner in which the chordwise integration is performed (see section 7.1) and because the current method can employ control points on the wing edges. Minor differences occur also in the corrections for the spanwise singularities. The method of Labrujere is also a kernel function method similar to the present method, but less so than Garner's method. The present method differs from the latter in the manner in which the chordwise integration is performed (see section 7.1 and table 7.3.1), in the method of spanwise integration (although the same set of integration points are used), and again because the current method is able to handle control points on the wing edges. For a further comparison of the Garner and Labrujere methods the reader is referred to Garner (1968).

The vortex lattice method is seen to give relatively poor results in comparison with the kernel function methods even though a large number of vortices were used. In fact the vortex lattice method does not seem to be converging to the correct answer as the number of panels is increased.

The vortex spline method is also seen not to be as accurate as the kernel function methods, although it is substantially better than the vortex lattice method for this particular wing.

9.3 The Warren 12 Wing

The so called Warren 12 wing is a swept, tapered wing shown in figure 9.3.1. The pressure modes in eqs. 5.5 - 5.7 are not entirely suitable near the kink at the center because the downwash modes that they create generally become infinite as the center section is approached except along the trailing edge. A procedure which has been adopted to overcome this difficulty is to introduce an artificial rounding of the planform near the center (Garner (1968)). Although the computer programs for the present method allow such a rounding to be done, it seemed to the author that other approaches would be easier and less subject to criticism. Specifically three different approaches were considered:

1. To use even values for *MM*, which automatically eliminates all control points on the centerline.
2. To use odd values for *MM*, but delete all the control points on the centerline.
3. To use odd values for *MM*, but delete all control points on the centerline except for the one at the trailing edge.

Procedure 1 is easily implemented, but, as will be discussed in section 10, it is the least efficient of any of the other two procedures. The second procedure is implemented by deleting all of the rows in the influence matrix that correspond to points on the centerline and by reducing *KK*, the number of spanwise modes by 2 (by deleting certain columns in the influence matrix). This results in an influence matrix which is still square. Procedure 3 is implemented in a similar way except that the trailing edge point is not eliminated. This results in a nonsquare influence matrix whose solutions are determined in the least squares sense. The equation solving program (Medan (1974)) was designed to easily accomodate procedures 2 and 3.

Figures 9.3.2 - 9.3.4 show certain results obtained using the above three procedures with 4 chordwise control points chosen according to the Wagner rule (eq. 8.1.2). Also shown are

results from Lagrujere (1968). All of these results are tabulated in table 9.3.1 along with a set of results using procedure 1 with the Multhopp chordwise control points (eq. 8.1.1). It can be seen that there is relatively little difference between the two columns in the table representing procedure 1. Thus results obtained with the current method as *MM* goes to infinity should be nearly the same as the results obtained by Labrujere as the amount of rounding goes to zero and *MM* goes to infinity. One can see from figures 9.3.2 - 9.3.4, however, that such is not the case. It is not known for certain which set of results is in error, but it seems that the current results are more likely to be correct since the answers extrapolated to *MM* equal to infinity do not vary appreciably with the chordwise or spanwise control point distribution and since a sufficient number of spanwise integration points was used (table 9.3.2). This discrepancy is probably not due to the rounding of the planform, but most likely is due to some numerical error or computer roundoff error, but, nevertheless, it should be resolved sometime.

An important result to observe is that the presence of the kink significantly and adversely affects the rate of convergence. In other words a much larger value of *MM* is required to obtain a given accuracy when a kink is introduced (compare figs. 9.1.3 and 9.3.2). Another result to note is that the rate of convergence of procedure 1 is significantly greater than for procedure 2 or 3. Furthermore procedure 3 is not better than procedure 2 as had been presupposed. A conclusion drawn from this study of the Warren 12 wing is that even though artificial rounding can be avoided, the problem of the kinked wing deserves more study.

PP	MM	JJ			
		31	63	127	255
3	3	1.80165 .65%	1.80226 .68%	1.80271 .71%	1.80294 .72%
	7	1.79824 .46%	1.79902 .50%	1.79950 .53%	1.79978 .55%
	15	1.79774 .43%	1.79857 .48%	1.79907 .51%	1.79934 .52%
4	3	1.79619 .34%	1.79583 .32%	1.79563 .31%	1.79542 .30%
	7	1.79030 .015%	1.78996 -.0035%	1.78973 -.016%	1.78955 -.026%
	15	1.78994 -.0046%	1.78874 -.072%	1.78860 -.079%	1.78840 -.091%
5	3	1.79635 .35%	1.79631 .35%	1.79628 .35%	1.79618 .34%
	7	1.79053 .028%	1.79127 .070%	1.79113 .060%	1.79104 .057%
	15	1.79044 .023%	1.79016 .0077%	1.79030 .015%	1.79015 .0071%
7	3	1.79631 .35%	1.79634 .35%	1.79632 .35%	1.79623 .35%
	7	1.79184 .10%	1.79088 .048%	1.79110 .060%	1.79100 .055%
	15	1.79130 .071%	1.79017 .0082%	1.79011 .0049%	1.79004 .00095%

TABLE 9.2.1. – THE LIFT COEFFICIENT CALCULATED FOR THE CIRCULAR WING. The numbers expressed as percentages are the errors determined from the exact result of 1.7900230 obtained by Jordan (1971).

PP	MM	JJ			
		31	63	127	255
3	3	1.00010	1.00010	1.00010	1.00010
	7	1.00026	1.00025	1.00024	1.00024
	15	1.00030	1.00029	1.00028	1.00027
4	3	1.00013	1.00013	1.00013	1.00013
	7	1.00040	1.00040	1.00039	1.00040
	15	1.00043	1.00050	1.00049	1.00048
5	3	1.00012	1.00012	1.00012	1.00012
	7	1.00037	1.00035	1.00036	1.00036
	15	1.00040	1.00043	1.00042	1.00042
7	3	1.00012	1.00012	1.00012	1.00012
	7	1.00035	1.00036	1.00036	1.00036
	15	1.00039	1.00044	1.00044	1.00044

TABLE 9.2.2. – THE VORTEX DRAG FACTOR CALCULATED FOR THE CIRCULAR WING.

PP	MM	JJ			
		31	63	127	255
3	3	.55349 .78%	.55164 .44%	.55039 .22%	.54947 .049%
	7	.55344 .77%	.55161 .44%	.55035 .21%	.54946 .047%
	15	.55345 .77%	.55161 .44%	.55034 .21%	.54944 .045%
4	3	.54951 .056%	.54950 .055%	.54947 .050%	.54941 .039%
	7	.54986 .12%	.54957 .068%	.54952 .058%	.54947 .049%
	15	.54940 .036%	.54959 .071%	.54948 .052%	.54942 .041%
5	3	.54926 .012%	.54926 .011%	.54924 .0077%	.54918 -.0034%
	7	.54850 -.13%	.54940 .038%	.54928 .015%	.54924 .0073%
	15	.54894 -.047%	.54924 .0082%	.54928 .015%	.54921 .0028%
7	3	.54903 -.031%	.54904 -.029%	.54917 -.0056%	.54913 -.012%
	7	.55096 .32%	.54842 -.14%	.54930 .018%	.54919 -.0016%
	15	.55061 .26%	.54891 -.053%	.54907 -.023%	.54918 -.0030%

TABLE 9.2.3. – THE PITCHING MOMENT ABOUT THE CENTROID CALCULATED FOR THE CIRCULAR WING. The reference chord is $16/(3\pi)(b/2)$. The numbers expressed as percentages are the errors determined from the exact result of 0.5491977 obtained by Jordan (1971).

PP	MM	JJ			
		31	63	127	255
3	3	-.30721 -.13%	-.30608 .24%	-.30531 .49%	-.30476 .67%
	7	-.30777 -.31%	-.30662 .063%	-.30583 .32%	-.30529 .50%
	15	-.30786 -.34%	-.30669 .038%	-.30590 .30%	-.30536 .47%
4	3	-.30593 .29%	-.30599 .27%	-.30601 .26%	-.30601 .26%
	7	-.30713 -.11%	-.30703 -.072%	-.30704 -.074%	-.30704 -.075%
	15	-.30694 -.041%	-.30725 -.14%	-.30722 -.13%	-.30722 -.13%
5	3	-.30576 .34%	-.30577 .34%	-.30577 .34%	-.30575 .35%
	7	-.30633 .16%	-.30671 .032%	-.30667 .047%	-.30666 .050%
	15	-.30660 .07%	-.30681 -.00051%	-.30681 .00080%	-.30680 .0044%
7	3	-.30564 .38%	-.30564 .38%	-.30572 .36%	-.30571 .36%
	7	-.30748 -.22%	-.30623 .19%	-.30668 .042%	-.30664 .056%
	15	-.30738 -.19%	-.30662 .061%	-.30672 .028%	-.30680 .0041%

TABLE 9.2.4. – THE CHORDWISE CENTER OF PRESSURE CALCULATED FOR THE CIRCULAR WING. The center of pressure is measured from the centroid and is in terms of the reference chord $\bar{c} = 16/(3\pi)(b/2)$. The numbers expressed as percentages are the errors determined from the exact result of -0.3068104 obtained by Jordan (1971).

PP	MM	JJ			
		31	63	127	255
3	3	1.77 11.1%	1.77 11.2%	1.77 11.2%	1.77 11.2%
	7	1.73 8.3%	1.73 8.5%	1.73 8.6%	1.73 8.7%
	15	1.69 6.3%	1.70 6.7%	1.70 6.9%	1.70 7.0%
4	3	1.76 10.5%	1.76 10.5%	1.76 10.5%	1.76 10.5%
	7	1.70 6.8%	1.70 6.8%	1.70 6.8%	1.70 6.8%
	15	1.68 5.3%	1.65 3.8%	1.66 3.9%	1.66 4.0%
5	3	1.76 10.6%	1.76 10.6%	1.76 10.6%	1.76 10.5%
	7	1.70 7.0%	1.71 7.2%	1.71 7.1%	1.71 7.1%
	15	1.68 5.7%	1.66 4.5%	1.67 4.8%	1.67 4.8%
7	3	1.76 10.6%	1.76 10.6%	1.76 10.6%	1.76 10.6%
	7	1.71 7.2%	1.71 7.1%	1.71 7.1%	1.71 7.1%
	15	1.68 5.5%	1.66 4.5%	1.67 4.6%	1.66 4.4%

TABLE 9.2.5. – THE TIP LIFT COEFFICIENT CALCULATED FOR THE CIRCULAR WING. The numbers expressed as percentages are the errors determined from the exact result of 1.5931 obtained by Jordan (1971).

PERSON	METHOD	ERROR IN CL	ERROR IN PITCHING MOMENT ABOUT CENTROID
MEDAN	Kernel function method PP=7, MM=15, JJ=255 Chordwise points from eq. 46	.0009%	-.0030%
GARNER (ref. 8)	Kernel function method PP=4, MM=11, JJ=95 Chordwise points from eq. 45	.015%	+.055%
LABRUJERE (ref. 8)	Kernel function method PP=4, MM=11 Chordwise points from eq. 45	.015%	+.019%
GIESING (ref. 24)	Vortex lattice method with 210 boxes	2.3%	+.38%
GIESING (ref. 24)	Vortex lattice with 504 boxes (252 unknowns)	2.8%	+.82%
MERCER (ref. 25, fig. 11)	Vortex spline	-.45%	-1.6%

TABLE 9.2.6. – A COMPARISON OF VARIOUS METHODS WHICH HAVE BEEN USED ON THE CIRCULAR WING.

QUANTITY	MM	PROCEDURE					
		1	1	2	3	NLR small rounding (ref. 8)	NLR large rounding (ref. 8)
		CHORDWISE CONTROL POINTS					
		EQ. 46	EQ. 45	EQ. 46	EQ. 46	EQ. 45	EQ. 45
Lift coefficient	6 or 7	2.8066	2.8063	2.8317	2.7876	--	--
	10 or 11	2.7895	--	2.8237	2.7904	--	--
	14 or 15	2.7794	2.7795	2.8123	2.7909	2.7373	2.7634
	22 or 23	2.7694	--	2.7922	2.7804	--	--
	30 or 31	2.7641	2.7648	2.7824	2.7742	2.7576	2.7632
Aerodynamic center (c=.72224b/2)	6 or 7	1.0228	1.0227	1.0105	1.0076	--	--
	10 or 11	1.0290	--	1.0229	1.0211	--	--
	14 or 15	1.0324	1.0322	1.0277	1.0266	1.0479	1.0445
	22 or 23	1.0359	--	1.0326	1.0321	--	--
	30 or 31	1.0376	1.0377	1.0352	1.0349	1.0429	1.0444
Local aerodynamic center at the centerline	6 or 7	.0244	.0244	.0000	.0124	--	--
	10 or 11	.0437	--	.0335	.0205	--	--
	14 or 15	.0559	.0550	.0481	.0382	.1502	.1509
	22 or 23	.0711	--	.0631	.0562	--	--
	30 or 31	.0807	.0809	.0733	.0679	.1356	.1498

TABLE 9.3.1. – A SUMMARY OF THE RESULTS OBTAINED FOR THE WARREN 12 PLANFORM.

MM	JJ	
	PRESENT	NLR
6	223	-
10	351	-
14	239	-
22	367	-
30	247	-
7	255	-
11	383	-
15	255	127
23	383	-
31	255	255

TABLE 9.3.2. – THE NUMBER OF SPANWISE INTEGRATION POINTS EMPLOYED IN OBTAINING THE RESULTS OF TABLE 9.3.1.

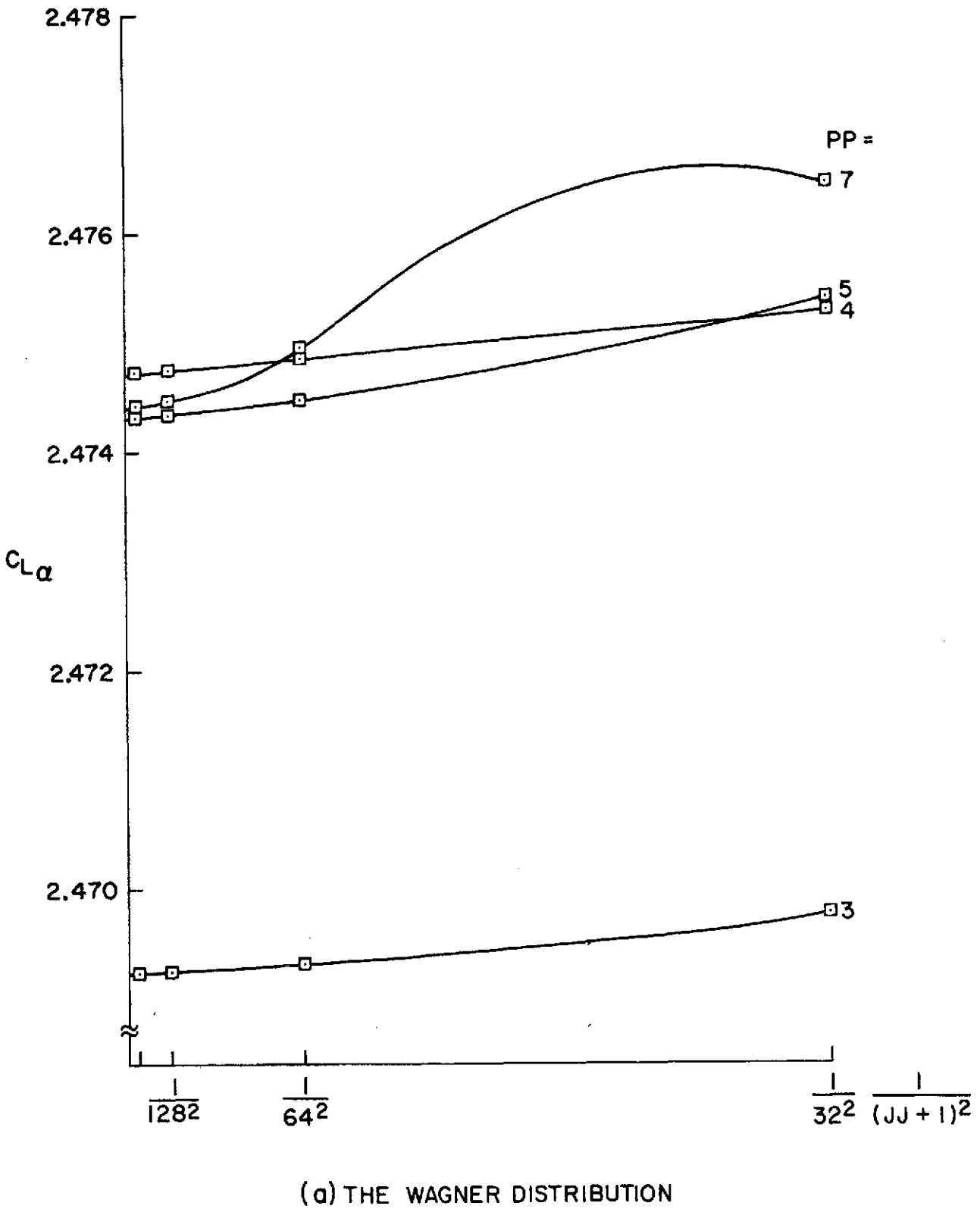

(a) THE WAGNER DISTRIBUTION

Figure 9.1.1. – The effects of the number of chordwise control points (PP), the control point distribution, and the number of spanwise integration points (JJ) on the predicted lift curve slope of the aspect ratio 2. rectangular wing. $MM = 7$. $\delta_0 = 1.$ for some cases.

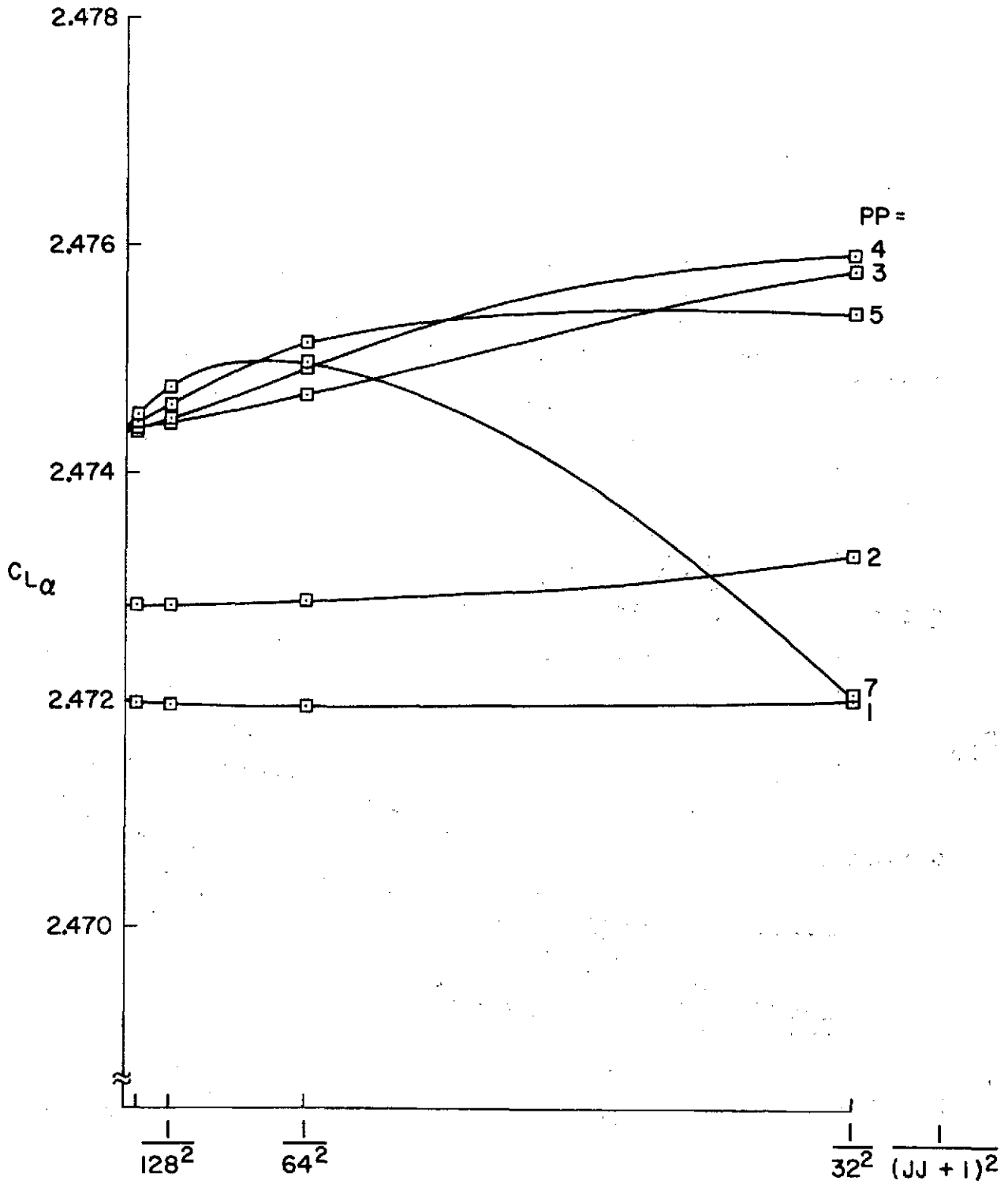

(b) THE MULTHOPP DISTRIBUTION

Figure 9.1.1. – Concluded.

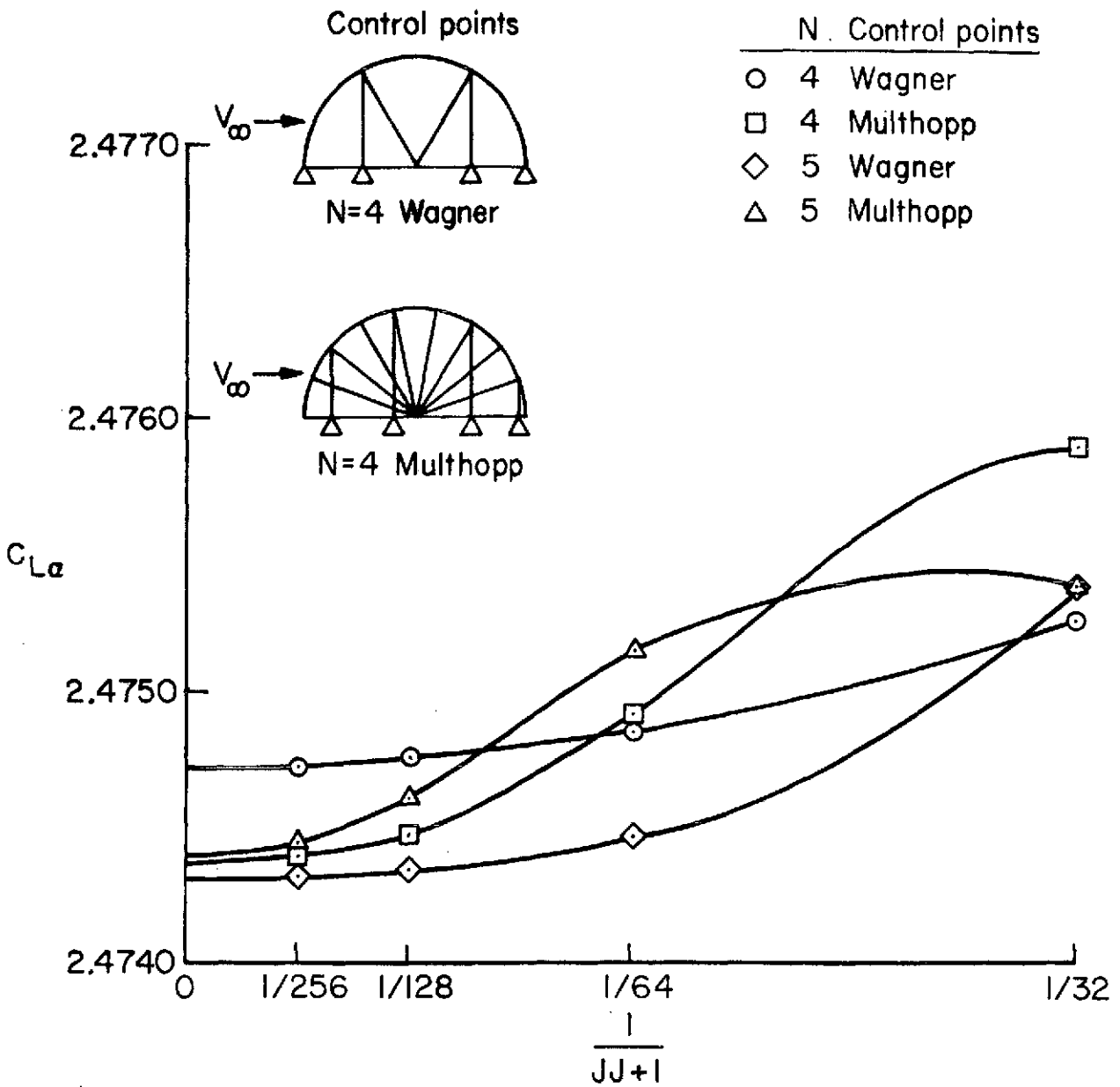

Figure 9.1.2. – The effects of the number of chordwise control points (*PP*), the control point distribution, and the number of spanwise integration points (*JJ*) on the predicted lift curve slope of the aspect ratio 2. rectangular wing.

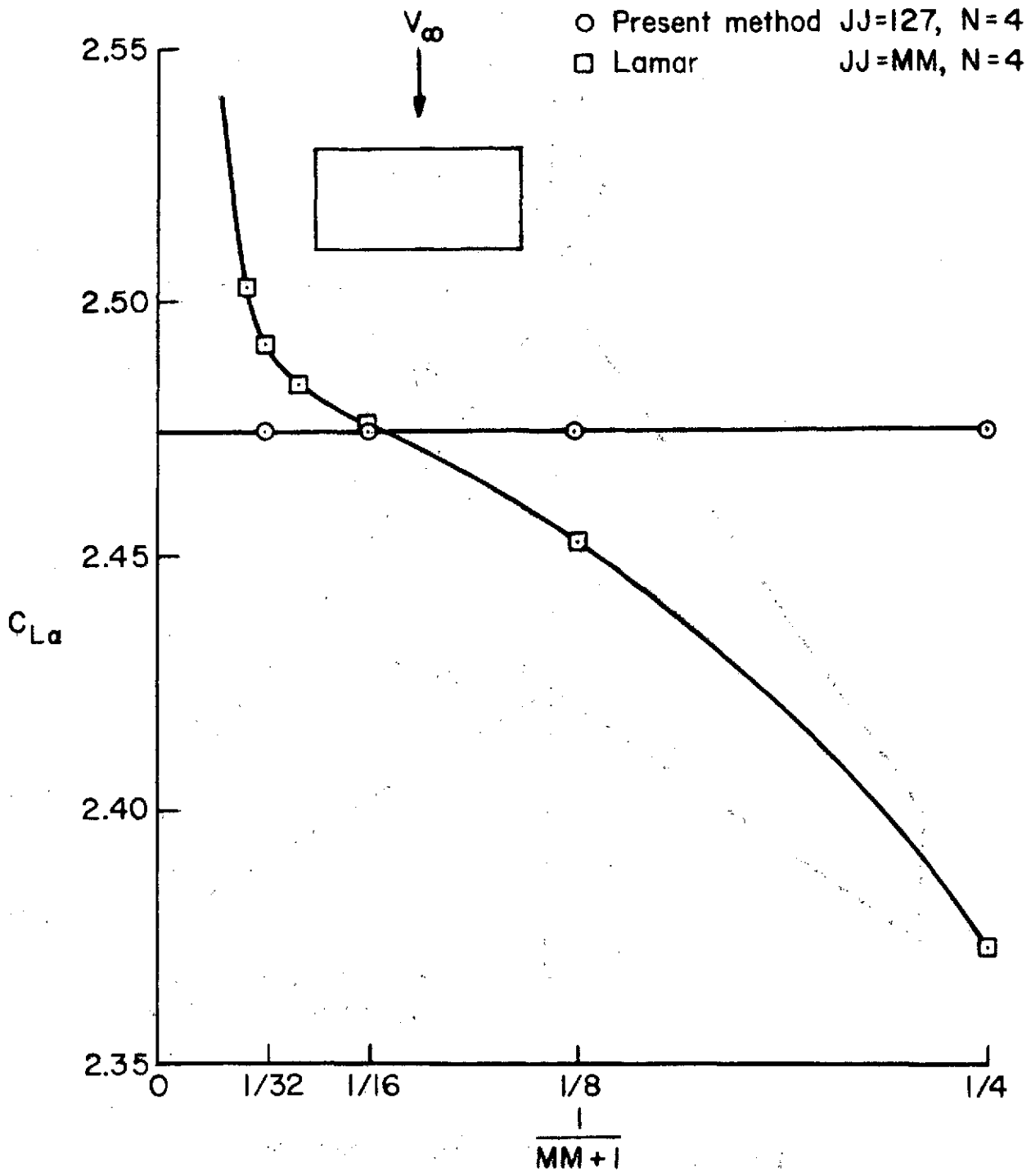

Figure 9.1.3. – The effect of revised integration procedures on predicting the lift curve slope of the aspect ratio 2. rectangular wing.

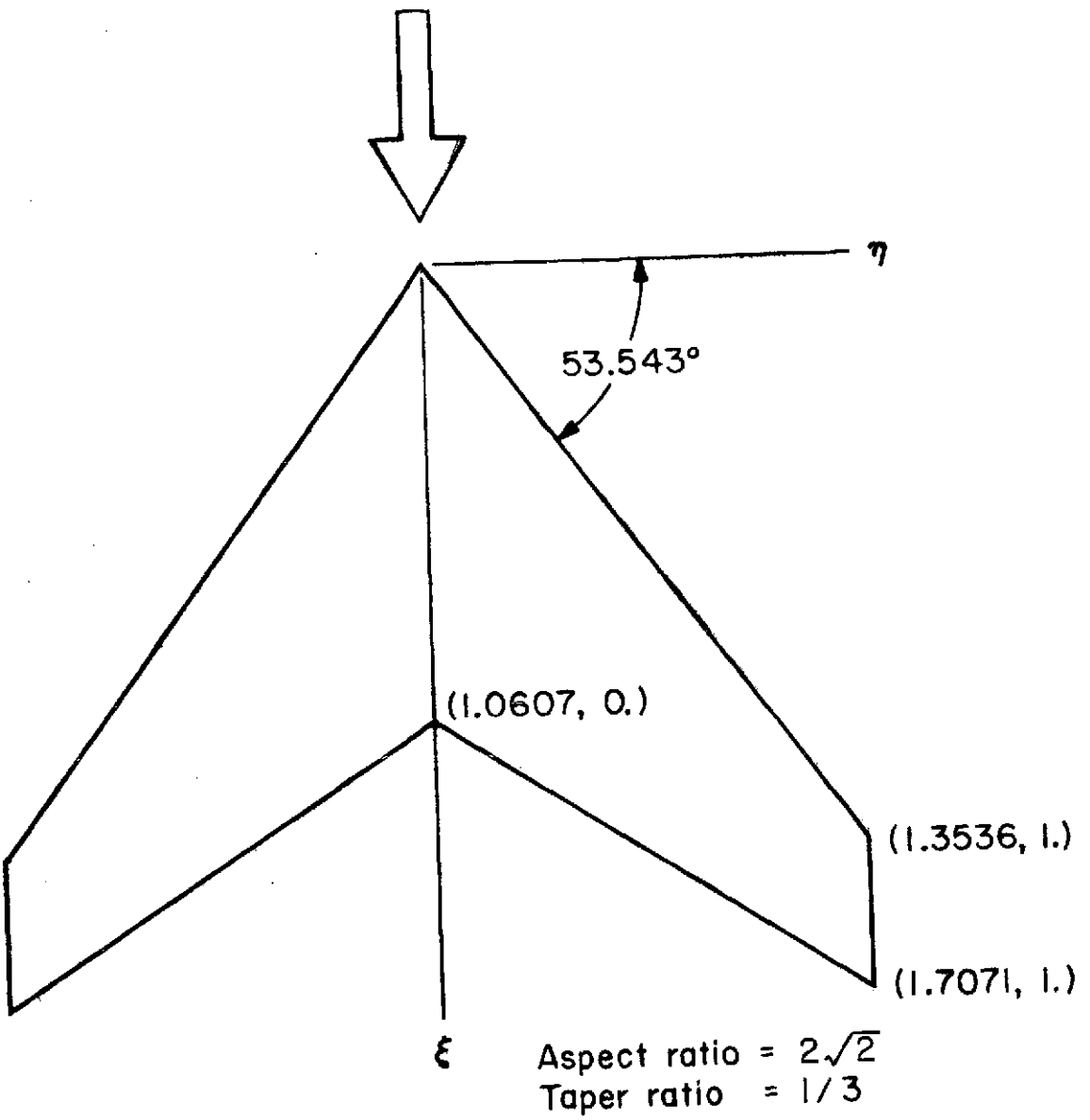

Figure 9.3.1. – The planform of the Warren 12 wing

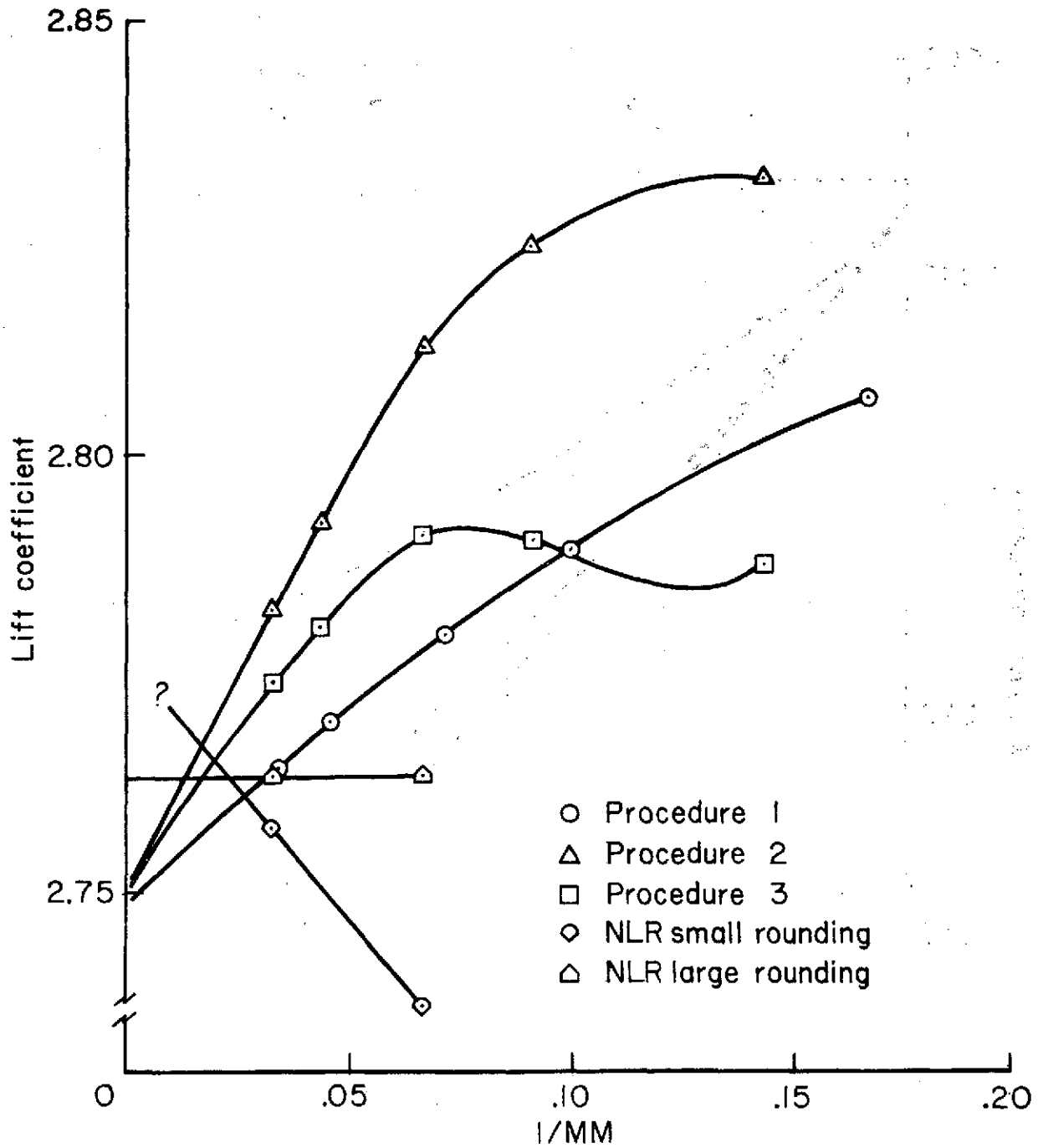

Figure 9.3.2. – The convergence of the lift coefficient of the Warren 12 planform with respect to the number of spanwise control points. $\alpha = 1$ radian.

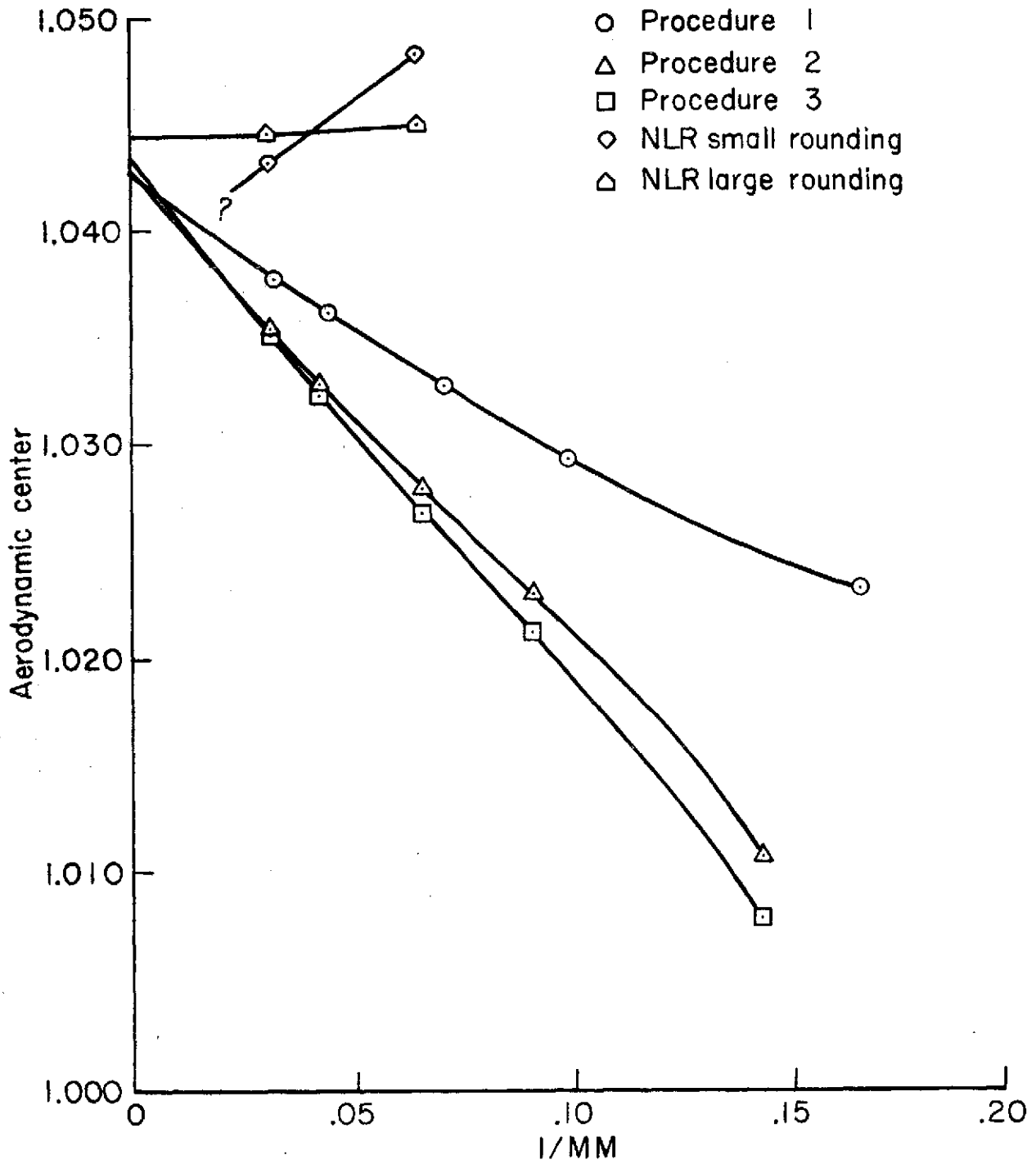

Figure 9.3.3. – The convergence of the aerodynamic center of the Warren 12 planform with respect to the number of spanwise control points. $\alpha = 1$ radian. $\bar{c} = 0.72224b/2$.

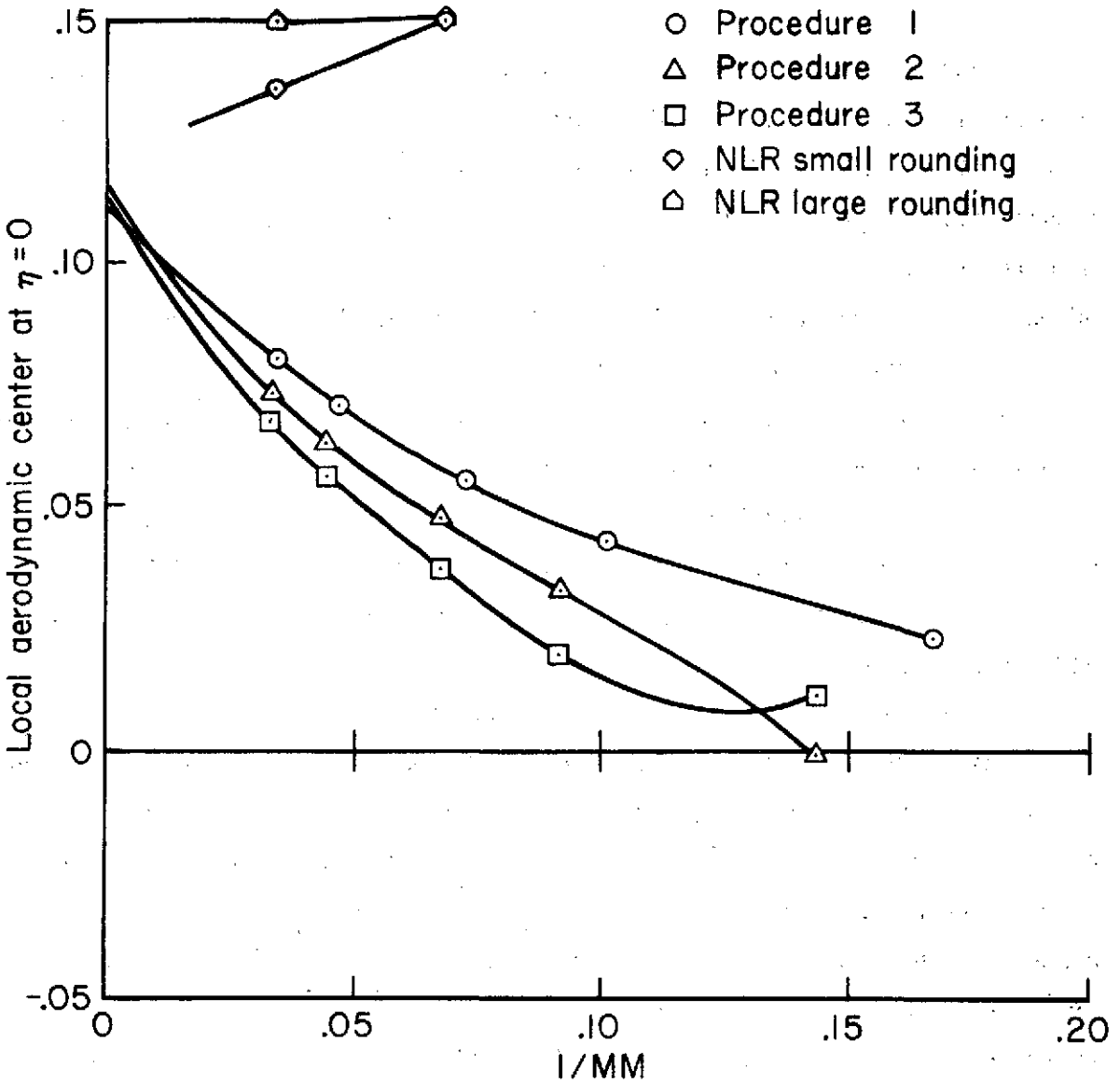

Figure 9.3.4. – The convergence of the local aerodynamic center at $\eta = 0$ of the Warren 12 planform with respect to the number of spanwise control points. $\alpha = 1.$ radian. The local aerodynamic center is measured relative to the local chord length and from the local ¼ chord line.

10. CONTROL POINT DUPLICATION

All methods similar to the one presented in this report have a certain natural advantage over other methods used in the analysis of thin wings. This advantage is that from a single influence matrix many other influence matrices, each corresponding to different values of the parameters *PP, MM, NN,* and *KK,* may be obtained. This results in significant computer cost savings because most of the cost associated with this method is encountered in calculating the influence matrices. This capability arises from the fact that the fundamental pressure modes are defined over the entire wing and without regard for where the control points are located.

Consider sets of spanwise control points chosen according to eq. 8.2.1. It can be seen from this equation that the set of points for some given value of *MM* are a subset of the control points for certain larger values of *MM*. For example the set of points for $MM = 3$ is identical to the set of even numbered points for $MM = 7$. Conversely, for all odd values of *MM* there exist one or more subsets which can be obtained from eq. 8.2.1. Table 10.1 lists various values of *MM* with the corresponding subsets.

Now consider the detailed structure of the influence matrix itself. Each row of the influence matrix corresponds to a single control point while each column corresponds to a single pressure mode. If *MM* were an odd number and $KK = MM$, then the influence matrix for $MM' = (MM - 1)/2 = KK'$ could be obtained by crossing out the set of $(MM + 1)/2$ rows corresponding to the odd-numbered spanwise control points and the $(MM + 1)/2$ columns corresponding to the spanwise pressure modes for which $K > (MM - 1)/2$. One could then use this influence matrix to determine the solution for the smaller value of *MM* and *KK*. Thus from the single influence matrix it is possible to extract multiple solutions which can then be used to study the convergence (i.e., as in figures 9.3.2 - 9.3.4). This duplication does not occur however, when *MM* is even and this is the reason using even values of *MM* is not as efficient as using odd values and is the reason for trying procedures 2 and 3 in the previous section.

In addition to the cases in which certain values of *MM* yield spanwise control points which are subsets of the control points for other, larger values of *MM*, there are also cases in which a significant number of the control points for one value of *MM* are identical to a significant number of the control points for a second value of *MM*. Table 10.2 lists some of these cases and the total number of control points involved.

This duplication of control points occurs not only for the spanwise control points, but also for the chordwise control points. Table 10.3 identifies certain advantageous combinations for both the Multhopp control points (eq. 8.1.1) and the Wagner control points (eq. 8.1.2). Although some propitious combinations occur for the Multhopp points, the most useful and effective combinations belong to the Wagner choice for the chordwise control points. This is the other advantage for the Wagner choice alluded to in the previous section.

This advantageous duplication of control points has been exploited in preparing the test cases for this report. For example the 36 cases for the circular wing were derived from only 4 influence matrices. One influence matrix was required for each value of JJ. Since symmetry allowed the control points for $\eta < 0$ to be disregarded, the number of control points for the 12 combinations of PP and MM in tables 9.2.1 - 9.2.5 was $(3 + 4 + 5 + 7) \cdot (2 + 4 + 8) = 266$. The number of points at which the pressure modes were calculated, however, was only $9 \cdot 8 = 72$ (see table 10.3, line 5 and table 10.2, line 7). Thus it can be seen that a large number of repetitive calculations can be avoided in a convergence study because of control point duplication.

MM	VALUES OF MM YIELDING SUBSETS
3	1
5	2,1
7	3,1
9	4,1
11	5,3,2,1
13	6,1
15	7,3,1
.	
.	
.	
31	15,7,3,1
.	
.	
.	
47	23,15,11,7,5,3,2,1

TABLE 10.1. – SUBSET RELATIONS FOR THE SPANWISE CONTROL POINTS.

VALUES OF MM	NUMBER OF SPANWISE CONTROL POINTS IN THE LOGICAL UNION
1,2,3,5,7,11	15
1,2,3,5,8,11,17	23
1,2,3,5,7,11,15,23	31
1,2,3,5,7,8,11,17,23,35	47

TABLE 10.2. – SETS OF VALUES OF *MM* FOR WHICH SIGNIFICANT DUPLICATION OF SPANWISE CONTROL POINTS OCCURS.

CONTROL POINT TYPE	VALUES OF PP	NUMBER OF CHORDWISE CONTROL POINTS IN THE LOGICAL UNION	EFFECTIVENESS RATIO (Σcol.2/col.3)
WAGNER	3,4	5	1.40
	3,5	5	1.60
	3,4,5	7	1.71
	3,4,7	7	2.00
	3,4,5,7	9	2.11
MULTHOPP	1,4	4	1.25
	1,2,7	7	1.43
	1,3,10	10	1.40
	1,2,4,7	10	1.40

TABLE 10.3. – SETS OF VALUES OF *PP* FOR WHICH SIGNIFICANT DUPLICATION OF THE CHORDWISE CONTROL POINTS OCCURS.

11. SUMMARY AND CONCLUSIONS

A method for solving the integral equation of subsonic, steady lifting surface theory has been presented. A new technique for performing the chordwise integration was given. This technique accounted for and took advantage of the fact that the chordwise integration cannot be independent of the spanwise integration. It was shown for two different planforms that the method requires fewer total integration points than two other methods while converging to the correct results.

The use of control points on the leading and trailing edges was discussed. Formulas to account for the irregularities in the spanwise integrand for control points on the wing edges were given. It was shown that the use of the Wagner chordwise locations, which includes the edge control points, is frequently advantageous to the usual Multhopp choice. It was shown that the advantages of the Wagner control points are that fewer spanwise integration stations are required and that there is greater control point duplication.

Wing edge kinks and cranks were discussed and methods alternative to the artificial rounding technique for handling the edge kinks and cranks were illustrated for a particular kinked wing. Although the alternative methods were possibly satisfactory, it was concluded that the problem of the kinked wing deserves more study.

Finally the report introduced and explained the concept of control point duplication, which allows studies of the convergence of the method with respect to the number of chordwise and spanwise control points to be conducted using considerably less computer time.

REFERENCES

Ashley, Holt and Landahl, Marten T. (1965): Aerodynamics of Wings and Bodies. Addison-Wesley, Reading, Mass.

Garner, H.C. (1966): Accuracy of Downwash Evaluation by Multhopp's Lifting-Surface Theory. R&M 3431, British A.R.C.

Garner, H.C.; Hewitt, B.L.; and Labrujere, T.E. (1968): Comparison of Three Methods for the Evaluation of Subsonic Lifting-Surface Theory. British A.R.C. R&M 3597.

Garner, H.C. and Miller, G.F. (1971): Analytical and Numerical Studies of Downwash over Rectangular Planforms. British National Physical Laboratory, Rept. Maths 99.

Giesing, J.P. (1968): Lifting Surface Theory for Wing-Fuselage Combinations. Rept. DAC-67212, Vol. 1, McDonnell Douglas Aircraft Co.

Hildebrand, F.B. (1956): Introduction to Numerical Analysis. McGraw-Hill Book Company, Inc., New York.

Hsu, Pao-Tan; and Weatherill, Warren H. (1959): Pressure Distribution and Flutter Analysis of Low-Aspect-Ratio Wings in Subsonic Flow. ASRL Tech. Rept. 64-3, Massachusetts Inst. Technol.

Jordan, P.F. (1967): Remarks on Applied Subsonic Lifting Surface Theory. WGLR-DGRR Annual Meeting, Karlsruhe, October 3-6.

Jordan, P.F. (1969): Wing-Edge Privot Points in Subsonic Lifting Surface Analysis. RIAS-TR-69-17C, Martin Marietta Corp., Baltimore, Maryland.

Jordan, P.F. (1971): The Parabolic Wing Tip in Subsonic Flow. AIAA Paper 71-10, AIAA 9th Aerospace Sciences Meeting, San Diego, Calif.; also Air Force Office of Scientific Research report AFOSR-TR-71-0075, Arlington, Va.

Labrujere (1968): See Garner (1968).

Lamar, John E. (1968): A Modified Multhopp Approach for Predicting Lifting Pressures and Camber Shape for Composite Planforms in Subsonic Flow. NASA TN D-4427.

Landahl, M. (1968): Pressure-Loading Functions for Oscillating Wings With Control Surfaces. AIAA J., vol. 6, no. 2, pp. 345-348.

Mangler, K.W. (1951): Improper Integrals in Theoretical Aerodynamics. British A.R.C. R&M 2424.

Mangler, K.W.; and Spencer B.F.R. (1952): Some Remarks on Multhopp's Lifting Surface Theory. British A.R.C. R&M 2926.

Medan, Richard T. (1973): Steady, Subsonic, Lifting Surface Theory for Wings with Swept, Partial Span, Trailing Edge Control Surfaces. NASA TN D-7251.

Medan, Richard T. (1973*b*): Geometry Program for Aerodynamic Lifting Surface Theory. NASA TMX-62,309.

Medan, Richard T. and Ray, K. Susan (1973*c*): Plotting Program for Aerodynamic Lifting Surface Theory. NASA TMX-62,321.

Medan, Richard T. and Ray, K. Susan (1973*d*): Boundary Conditions Program for Aerodynamic Lifting Surface Theory. NASA TMX-62,323.

Medan, Richard T. and Ray, K. Susan (1973*e*): Influence Matrix Program for Aerodynamic Lifting Surface Theory. NASA TMX-62,324.

Medan, Richard T. and Lemmer, Opal J. (1974): Equation Solving Program for Aerodynamic Lifting Surface Theory. NASA TMX-62,325.

Medan, Richard T. and Ray, K. Susan (1974*b*): Normal Loads Program for Aerodynamic Lifting Surface Theory. NASA TMX-62,326.

Mercer, J.E.; Weber, J.A.; and Lesferd, E.P. (1973): Aerodynamic Influence Coefficient Method Using Singularity Splines. AIAA Paper 73-123, AIAA 11th Aerospace Sciences Meeting, Wash., D.C., Jan. 10-12, 1973.

Multhopp, Hans (1950): Methods for Calculating the Lift Distribution of Wings (Subsonic Lifting-Surface Theory). British A.R.C., R&M 2884.

Rossiter, Patricia J. (1969): The Linearised Subsonic Flow over the Centre-Section of a Lifting Swept Wing. British A.R.C. R&M 3630.

Wagner, Seigfried (1967): Beitrag zum Singularitatenverfahren der Tragflächentheorie bie Inkompressibler Strömung. Ph.D. Thesis, Technical University Munich.

Zandbergen, P.J.; Labrujere, Th. E.; and Wouters, J.G. (1967): A New Approach to the Numerical Solution of the Equation of Subsonic Lifting Surface Theory. National Aerospace Lab. Rept. NLR-TR-G-49, The Netherlands.